https://doi.org/10.5194/egusphere-2025-6351
Preprint. Discussion started: 19 March 2026

Assessing the Impact of Freshwater Fluxes from Major Rivers on the Atlantic Ocean

Louis Kern[1], Thomas Vaujour[1], Julia Pfeffer[1], Andrea Storto[2], Camille Szczypta[3], Gilles Garric[4], Claire Sirere[4], Gilles Larnicol[1], Chunxue Yang[2], Romain Bourdalle-Badie[4], Stéphanie Guinehut[4]

[1] Magellium, 1 rue Ariane, Toulouse, France
[2] CNR-ISMAR, Rome, Italy
[3] EDF, Toulouse, France
[4] Mercator Ocean International, Toulouse, France

Correspondence to: Louis Kern (louis.kern@magellium.fr)

Abstract. This study evaluates the impact of freshwater fluxes on the Atlantic Ocean. The river discharge has been estimated at the outlet of 18 major rivers flowing into the Atlantic by solving the water mass balance equation at the river basin scale. In this approach, water storage changes are evaluated with satellite gravimetry measurements. In contrast, atmospheric fluxes (i.e., precipitation, evapotranspiration) are assessed with atmospheric reanalyses, in situ measurements from a global network of rain gauges, or a global hydrological model. The river discharge estimated with the water mass balance is consistent with independent river gauge measurements across all South American rivers, in particular the Amazon, where the annual and monthly climatology can be estimated with an error of less than 5 % when compared with in situ measurements. Larger discrepancies are observed for other basins, likely due to uncertainties in the precipitation and evapotranspiration fluxes. When climatological estimates of the river discharge are replaced by the water mass balance approach in ocean model simulations, a decrease in the sea surface salinity bias is observed at the outlet of the Amazon and across the whole Atlantic. The water mass balance approach can bring new observational constraints on freshwater fluxes flowing from the continent to the ocean, but is not universally reliable due to potential biases in atmospheric flux estimates. When combined with in situ measurements or hydrological model predictions, the water mass balance approach can enhance freshwater flux quantification, leading to improved ocean model simulations near major river outlets. In particular, the enhanced river runoff dataset significantly reduces salinity biases, with associated changes in reduced vertical stratification, enhanced upper ocean circulation, and meridional transports.

1 Introduction

Freshwater fluxes play a critical role in shaping ocean dynamics, primarily by inducing regional density variations through changes in salinity. These freshwater inputs, originating from river discharge, precipitation, and ice melt, influence upper-ocean stratification, circulation, and air-sea interactions. In regions such as the eastern tropical North Atlantic, freshwater fluxes drive seasonal and interannual variability in sea surface salinity (SSS), modulating the upper-ocean buoyancy balance and affecting ocean-atmosphere coupling (Thouvenin-Masson et al., 2024). On a broader scale, major river systems such as the Amazon have been shown to affect global thermohaline circulation, heat distribution, and atmospheric convection (Huang and Mehta, 2010; Jahfer et al., 2017).

https://doi.org/10.5194/egusphere-2025-6351
Preprint. Discussion started: 19 March 2026

In addition to salinity regulation, freshwater fluxes contribute to ocean mass redistribution, influencing both regional and global sea level. Mass anomalies caused by land-to-ocean water exchanges propagate rapidly—within ~10 days—across ocean basins through barotropic waves (Dobslaw and Thomas, 2007). Changes in terrestrial water storage, driven by natural variability and anthropogenic activities, have been linked to sea level changes ranging from a few millimeters to several centimeters on time scales from days to decades (Cáceres et al., 2020; Hamlington et al., 2020; Pfeffer et al., 2022). As the global hydrological cycle intensifies with climate change (Fournier et al., 2023), understanding the variability of these fluxes becomes essential for accurate ocean state estimation and climate prediction.

Despite their importance, freshwater fluxes are often poorly represented in ocean models. Many operational systems and reanalyses (e.g., (Storto et al., 2019)) rely on climatological or highly simplified river discharge datasets, which fail to capture the temporal variability and long-term trends critical for accurate simulation of ocean salinity, circulation, and sea level. This limitation affects not only the realism of ocean simulations but also the fidelity of coupled atmosphere-ocean models used for climate forecasting (Sausen et al., 1994). Incorporating more realistic, time-varying freshwater inputs has been shown to improve both regional sea level simulations and the representation of key climate signals (Tajouri et al., 2024).

Traditional estimates of river discharge rely heavily on in situ stream gauges, which suffer from uneven spatial coverage and are often located far upstream from river mouths (Dai and Trenberth, 2002). Additionally, access to gauge data is restricted in many regions due to institutional, political, and economic constraints. These limitations hamper efforts to consistently quantify freshwater fluxes into the ocean at global scales.

Satellite gravimetry offers a promising alternative. Observations from the GRACE (Tapley et al., 2004) and GRACE-FO (Landerer et al., 2020) missions enable monitoring of large-scale water mass redistribution across the Earth system. By combining satellite-derived terrestrial water storage anomalies with vertical atmospheric fluxes—precipitation and evapotranspiration—from reanalyses or land surface models, river discharge can be estimated using the Water Mass Balance (WMB) approach. This method has been used to estimate monthly and seasonal freshwater fluxes from river basins to continental scales, showing critical sensitivity to the choice of atmospheric reanalyses used to estimate vertical fluxes (Syed et al., 2005, 2009). Validation efforts in the Amazon basin have demonstrated good agreement between WMB-derived river discharges and in situ measurements at Óbidos, both in terms of seasonal variability and long-term trends (Chen et al., 2020). Importantly, this approach can also help identify biases in atmospheric flux estimates—especially evapotranspiration—that affect freshwater balance accuracy.

In this study, we apply the WMB approach to estimate river discharge from 18 major river basins draining into the Atlantic Ocean. These estimates are validated against available in situ river gauge data. The WMB-derived discharges are then used as freshwater forcing in ocean model simulations. Simulated sea surface salinity is compared to independent verifying data, such as EN4 objective analyses , to evaluate the accuracy of the approach and to assess the impact of land-to-ocean freshwater fluxes on the Atlantic Ocean at seasonal to interannual timescales.

https://doi.org/10.5194/egusphere-2025-6351
Preprint. Discussion started: 19 March 2026

2 Data and Methods

2.1 Study area

The objective of this study is to assess the impact of freshwater fluxes on the Atlantic Ocean by estimating river discharge using the Water Mass Balance (WMB) approach. This method combines satellite gravimetry data from the GRACE and GRACE-FO missions with atmospheric or land surface reanalyses to quantify river discharge.

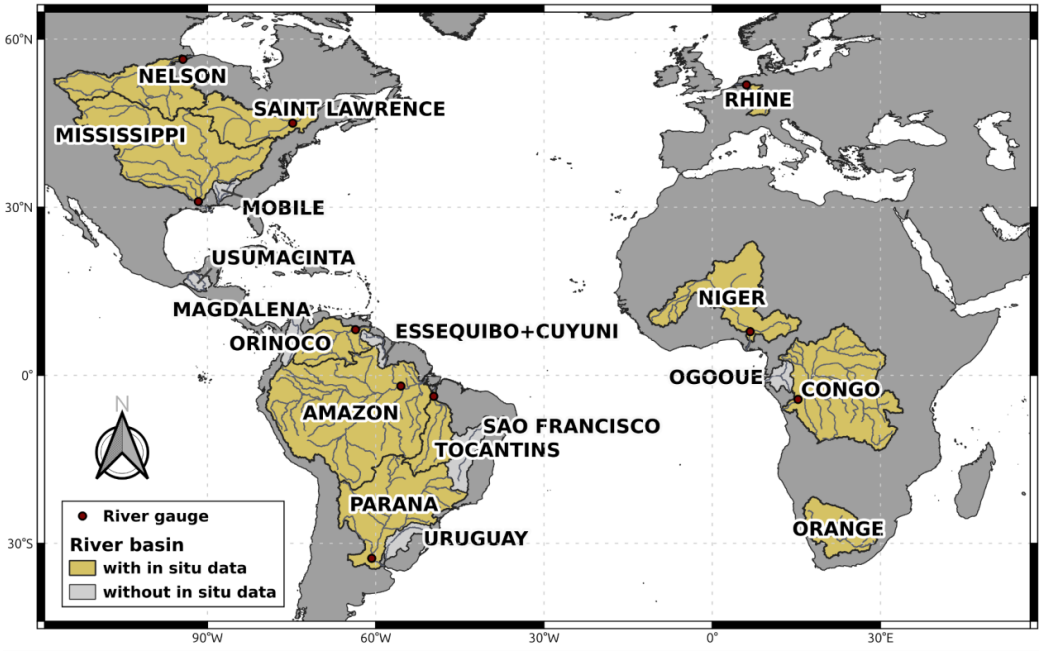

Figure 1: Map of the 18 selected rivers with their associated catchment areas. The yellow areas represent river basins where in situ data have been used for quality assessment, with the locations displayed of the river gauges shown as red dots. Light grey areas represent river basins where no in situ measurements were available over the observation period (January 2003 - December 2020).

To ensure a comprehensive coverage of all major rivers discharging into the Atlantic Ocean, all rivers with an average discharge exceeding 2,000 m^3/s were initially identified using data from the HydroRIVERS database (Lehner and Grill, 2013). From this preliminary selection, only the rivers with a catchment area larger than 100,000 km^2 were retained, in order to align with the spatial resolution of GRACE and GRACE-FO measurements, which is approximately 300 × 300 km. This process resulted in the selection of 18 river basins distributed across four continents—North and South America, Africa, and Europe—and encompassing a wide range of climatic regimes in terms of precipitation and temperature (Fig. 1).

The main characteristics of the selected basins are summarized in Table 1. River names and outlet locations are taken from the HydroRIVERS database (Lehner and Grill, 2013). Notably, the Essequibo and Cuyuni Rivers were combined due to their shared outlet. Although the Orange River has an average discharge below the 2,000 m^3/s threshold (~300 m^3/s), it was included in the final selection due to its extensive catchment area, which ensures compatibility with the spatial resolution of satellite gravimetry data. The basin areas are extracted from the Major River Basin database (GRDC, 2020).

https://doi.org/10.5194/egusphere-2025-6351
Preprint. Discussion started: 19 March 2026

94

River Name	Latitude of the river outlet	Longitude of the river outlet	Basin area (km²)	Mean discharge at outlet (m^3/s)	In-situ measurements	Mean precipitation (m/years)
Amazon	-0.67	-51.10	5965894	205604	GRDC	2.38
Congo	-6.07	12.48	3705225	39637	HyBAM	1.44
Orinoco	8.58	-60.98	941419	37053	HyBAM	2.47
Mississippi	29.19	-89.28	3240620	21894	GRDC	0.85
Parana	-33.93	-58.54	2646513	18311	GRDC	1.28
Saint-Lawrence	46.80	-71.21	1053299	12344	GRDC	1.03
Tocantins	-2.20	-49.41	772469	11408	Dai&Trenberth	1.57
Magdalena	11.02	-74.79	260737	7248	-	3.38
Niger	4.41	6.06	2122995	6859	GRDC	0.55
Uruguay	-32.93	-58.11	266134	6423	-	1.68
Ogooue	-1.00	8.92	215213	4805	-	1.83
Cuyuni and Essequibo	6.45	-58.59	154857	3935	-	2.17
Usumacinta	18.56	-92.67	127388	3583	-	1.80
Nelson	56.93	-92.75	1106520	2750	GRDC	0.62
Sao Francisco	-10.46	-36.42	637202	2697	GRDC	0.75
Rhine	51.96	4.16	163122	2451	GRDC	1.07
Mobile	30.70	-88.04	112528	2100	-	1.29
Orange	-28.60	16.47	977322	310	GRDC	0.37

95 **Table 1: Selected basins characteristics. River outlet coordinates are given in degrees. Mean discharge at the outlet**
96 **corresponds to the long-term average discharge from the Hydro Rivers dataset. The mean precipitation corresponds to**
97 **ERA5 precipitations averaged over the basin area during the 2002—2019 period.**

98 **2.2 In- Situ Measurements of the River Discharge**

99 The Global Runoff Data Centre (GRDC) Data Download Portal offers the most comprehensive, quality-controlled database of
100 river discharge observations, comprising daily and monthly time series from over 10,800 gauging stations along approximately
101 7,000 rivers worldwide (Federal Institute of Hydrology, 2024). The database incorporates various in situ measurement techniques
102 as described by (Dobriyal et al., 2017). Typically, manual discharge measurements are collected at different river stages using
103 devices such as current meters, Acoustic Doppler Current Profilers (ADCPs), or other flow-measuring instruments. For each stage
104 (water level), the corresponding discharge is recorded. A rating curve—often modeled as a power-law function—is then fitted to

https://doi.org/10.5194/egusphere-2025-6351
Preprint. Discussion started: 19 March 2026

these data, enabling continuous estimation of river discharge from continuously monitored stage values. However, this method carries inherent uncertainties, typically around 15%, and is both time-consuming and labor-intensive (Crétaux et al., 2016). Establishing and maintaining in situ gauging stations is therefore costly, which limits their deployment primarily to main river stems, resulting in sparse coverage and limited data availability for remote rivers and tributaries. Moreover, the number of active gauges in the GRDC database has significantly declined since the 1980s, with only 14% remaining active by 2020 (Elmi et al., 2024). For example, just 2,200 stations have reported discharge data beyond 2015. While some stations provide daily data, others report only monthly values.

To enhance the coverage, the GRDC database has been complemented by the HYBAM (HYdro-géochimie du Bassin AMazonien) project (Catalogue – Hybam, 2025), which provides monthly in situ discharge measurements using the ADCP method (Dobriyal et al., 2017) for 17 stations located in South America and the Congo Basin.

In order to avoid gaps in the Tocantins dataset from GRDC, discharge estimates from (Dai, 2017) have been used as reference. In situ measurements were acquired at the Tuvcurui station located the closest to the river mouth. Temporal gaps are filled with data from nearby gauges if available and otherwise with a regression based on a hydrological model. Additional corrections are detailed in (Dai et al., 2009).

Combining the GRDC, HYBAM and Dai&Trenberth datasets, in situ discharge measurements were available for 11 out of the 18 selected rivers since 2000 (Fig. 2). The Magdalena, Usumacinta, Essequibo, Cuyuni, São Francisco, Uruguay, and Ogooué rivers were not sampled since 2000. The Orange River had the longest observation period, lasting 90 years until today, while the Niger River had only 13 years of intermittent data since 2002. Among the 11 rivers sampled with in situ observations, the Orange, Rhine, Nelson, Saint Lawrence, Paraná, Orinoco, Congo, and Amazon rivers all benefited from long, continuous discharge records spanning over the 16 years of the period covered by the WMB approach using GPCC precipitation and ISBA-CTRIP evapotranspiration.

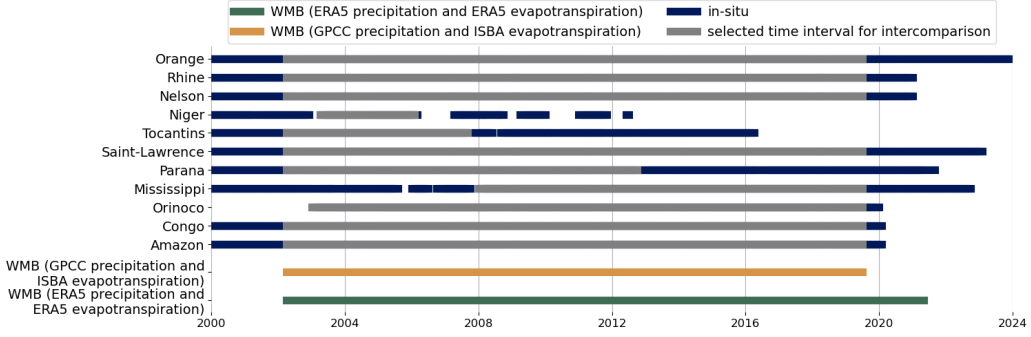

Figure 2: Availability of river discharge measurements through time. Blue lines represent periods with available in situ discharge data. Grey lines indicate the longest continuous interval with monthly in situ data, used for comparison with WMB results. The orange line shows the time span covered by the WMB approach using GPCC precipitation and ISBA evapotranspiration, bounded by the launch of the GRACE satellites (start) and the availability of the ISBA-CTRIP model (end). The green line shows the WMB time span based on ERA5 precipitation and evapotranspiration.

2.3 The Water Mass Balance Approach

The river discharge can be estimated using the water mass balance equation, expressed as:

https://doi.org/10.5194/egusphere-2025-6351
Preprint. Discussion started: 19 March 2026

$$\frac{dS}{dt} = P - ET - R \quad (1)$$

where dS/dt are the changes in land water storage in time, P the precipitation, ET the evapotranspiration and R the river discharge.

Terrestrial Water Storage (TWS) anomalies have been estimated from April 2002 to August 2023 at monthly timescales and with a spatial resolution of 1 degree using an ensemble of GRACE and GRACE-FO solutions derived from (Blazquez et al., 2018). The GRACE and GRACE-FO ensemble comprises 120 solutions, allowing the estimation of uncertainties associated with different processing strategies and geophysical corrections needed for hydrological applications. The ensemble is based on coefficients of the Earth's gravitational potential anomalies estimated by five centers (CNES, CSR, JPL, GFZ, ITSG). A large variety of post-processing corrections are applied to the ensemble, including two models of the geocentre motions (Lemoine and Reinquin, 2017; Sun et al., 2016), three models of the oblateness (C20) of the Earth (Cheng et al., 2013; Lemoine and Reinquin, 2017; Loomis et al., 2019), and two GIA models (Caron et al., 2018; Peltier et al., 2018). To reduce the anisotropic noise, decorrelation filters, called DDK filters (Kusche et al., 2009), are applied to GRACE solutions, using two different orders (DDK3 and DDK6) corresponding to different levels of filtering. The ensemble of 120 solutions results from combining these five processing centers, two geocenter models, three oblateness models, two GIA corrections, and two filters.

The monthly TWS anomalies are then averaged at river basin scale. To compute the first derivative of TWS changes (dS/dt), the GRACE and GRACE-FO time series need to be processed in order to fill data gaps ranging from 1 (satellite operations) to 11 (time gap between the two missions) months. In our dynamic interpolation, we first remove the seasonal terms (annual and semi-annual sinusoids) and linear trends estimated by least squares adjustments, we then use linear interpolation to reconstruct residual TWS times series at the start of each month, and finally we add the seasonal terms and linear trends back to the reconstructed TWS time series. The first derivative of TWS changes (dS/dt) can then be computed as the difference between two consecutive TWS estimates. As noted by (Chen et al., 2020), it is important to interpolate terrestrial water storage (TWS) anomalies to the start of each month. This ensures that the differentiation between consecutive months yields a first-order estimate of TWS changes that is consistent with precipitation and evapotranspiration data averaged over calendar months.

The precipitation (P) is averaged by calendar month and by basin, using the GPCC observational product (Schneider et al., 2015) spanning over 1980-2022 or with the ERA5 reanalysis (Hersbach et al., 2020) spanning over 1980-today. The mean evapotranspiration is estimated with the ERA5 reanalysis spanning over 1980-today, or with the ISBA-CTRIP hydrological model (Decharme et al., 2019) spanning over 1979-2019. Two combinations of river discharge (R) are then calculated based on the difference between the net precipitation (P-ET) and the first derivative of terrestrial water storage changes (dS/dt) for each river basin. The first combination uses ERA5 precipitation and evapotranspiration and will be referred to hereafter as WMB1. The second uses GPCC precipitation together with ISBA-CTRIP evapotranspiration and will be referred to hereafter as WMB2. It may be noted that the ISBA-CTRIP hydrological model is forced with GPCC precipitation, ensuring consistency at the model scale, between the atmospheric fluxes considered. The combination using ERA5 atmospheric fluxes spans over the full GRACE and GRACE-FO observation period considered in this study (i.e. April 2022 to May 2021), while the combination using GPCC and ISBA-CTRIP spans over April 2002 until July 2019.

https://doi.org/10.5194/egusphere-2025-6351
Preprint. Discussion started: 19 March 2026

2.4 Ocean Model Simulations

To assess the impact of river discharge estimates on ocean model simulations, this study employs the NEMO ocean model (version 4.0.7, (Madec et al., 2017)), which includes the sea-ice dynamic and thermodynamic model SI^3. The model is configured on the ORCA1 grid, featuring a horizontal resolution of 1° with enhanced resolution in the tropical regions, and 75 vertical depth levels with partial steps (Bernard et al., 2006). The surface boundary conditions are computed using the CORE bulk formulas (Large and Yeager, 2009), implemented via the AEROBULK package (Brodeau et al., 2017). Meteorological forcing data are derived from the ECMWF ERA5 atmospheric reanalysis (Hersbach et al., 2020) at hourly frequency. The model setup is the same as the CIGAR reanalysis (Storto and Yang, 2024). It incorporates a 3-band RGB scheme for net shortwave radiation, with extinction coefficients based on a monthly climatology of chlorophyll. Vertical mixing is parameterized using the TKE scheme (Gaspar et al., 1990), and tracers and momentum are diffused using Laplacian and bi-Laplacian operators, respectively.

The experiments we present do not include any data assimilation or bias correction. This approach allows us to evaluate the impact of the river discharge dataset without any interplay with observations. The experiments cover the period from January 2003 to December 2020 and are all initialized from the same initial conditions, taken from the CIGAR reanalysis.

We configured several experiments to assess the impact of different river discharge inputs on ocean modeling. The reference experiment (REF) uses the standard NEMO monthly climatology of river discharge from the (Dai and Trenberth, 2002) dataset, as compiled by (Bourdalle-Badie and Treguier, 2006). A second experiment (J5) uses daily varying runoff from the JRA-55-do dataset (Tsujino et al., 2018), based on a bias-corrected land component of the JRA-55 atmospheric reanalysis (using ERA5 as atmospheric forcing as all the other experiments). In addition, we conducted four experiments that incorporate Water Mass Balance (WMB)-derived discharge estimates in place of the monthly climatology for the Atlantic Ocean. Experiments A1 and A2 replace the discharge climatology with WMB estimates for all 18 major rivers listed in Table 1. A1 uses precipitation and evapotranspiration from GPCC and ISBA, respectively, while A2 uses both fields from the ECMWF ERA5 reanalysis. Experiments S1 and S2 focus on isolating the impact of the Amazon, Orinoco, and Tocantins rivers, which show high-confidence results under the WMB approach. In these experiments, WMB estimates are used only for those three rivers, while discharge from all other rivers follows the reference climatology. As with A1/A2, S1 uses GPCC and ISBA, while S2 uses ERA5.

To adopt the WMB-derived dataset in the NEMO simulations, the 18 major river basins have been remapped onto the NEMO ORCA1 grid through conservative remapping, using the local spread of the runoff within the coastlines of the pertinence of each river drainage basin, proportional in area to the monthly climatology of (Bourdalle-Badie and Treguier, 2006).

3 Quantification of freshwater fluxes over 18 major rivers

3.1. Comparison of river discharge estimates at the Obidos station

The Amazon River has a mean discharge more than four times greater than that of the next largest river flowing into the Atlantic—the Congo River (Table 1). Accurately estimating the Amazon River discharge is therefore crucial for assessing the impact of freshwater fluxes on the ocean. This assessment is carried out by comparing river discharge estimated with the WMB approach to in situ measurements at the Óbidios gauging station, located approximately 500 km upstream of the Amazon delta (Fig. 3). To ensure consistency between the WMB-derived and observed discharge, TWS anomalies, precipitation (P), and evapotranspiration (ET) were averaged over the station drainage area, as defined by the Global Runoff Data Centre (GRDC).

https://doi.org/10.5194/egusphere-2025-6351
Preprint. Discussion started: 19 March 2026

211

212 Overall, excellent agreement can be observed between the WMB estimates and in situ measurements acquired at the Obidios gauge,
213 with Pearson's correlation coefficient reaching 0.87 when ERA5 is used to constrain atmospheric fluxes (WMB1) and 0.88 when
214 GPCC and ISBA-CTRIP are used (WMB2) (Fig. 3). The average river discharge (1.734e+5 m^3/s) is well captured by the WMB
215 approach, with a difference of only +2 % in WMB1 and -3% in WMB2.

216

217 Differences between both WMB approaches appear in their ability to retrieve the seasonal cycle amplitude. While excellent
218 agreement (+ 5%) with in situ data is retrieved in WMB1, more significant discrepancies occur in WMB2, leading to an
219 overestimation of the annual cycle of the river discharge by 46% when compared with in situ data. The phase of the seasonal cycle
220 is also well captured by the WMB approach. The months of the highest and lowest discharge are May and November, both for in
221 situ measurements and the WMB1 approach. By comparison, the highest discharge is two months late when comparing WMB2 to
222 in situ measurements.

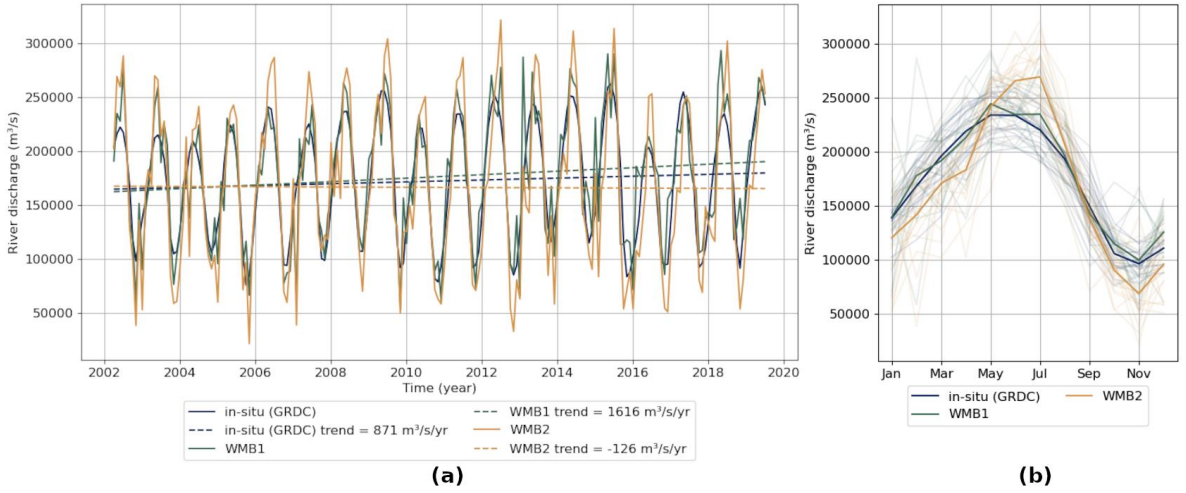

223

224 **Figure 3: Discharge values at Obidos-Linigrafo station on the Amazon. In situ measurements are taken from the GRDC dataset, WMB1**
225 **refers to estimates from the WMB approach using ERA5 for precipitation and evapotranspiration. WMB2 refers to the WMB approach**
226 **using GPCC for precipitation and ISBA for evapotranspiration. (a) displays monthly discharge values as solid lines, and the**
227 **corresponding decadal trends as dashed lines. (b) shows seasonal cycles, with the solid line representing the mean seasonal cycle for each**
228 **dataset.**

229

230 Linear trends have also been computed by ordinary least square adjustment over April 2002—December 2019. A small decadal
231 trend of 871 m3/s/yr is observed in in situ river discharge measurements, overestimated with WMB1 and underestimated with
232 WMB2. It may however be noted that this trend is not significant in regard with the annual and interannual variability of the
233 Amazon discharge, and these values are likely to change a lot depending on the observation period considered. Both WMB
234 approaches exhibit stronger high frequency variability compared to in situ measurements with extreme events more marked with
235 WMB2 than WMB1.

236

237 The WMB approach is further evaluated using several performance metrics: percent bias (PBias) for the temporal mean, the
238 correlation coefficient (R), the variability ratio (γ), and the modified Kling-Gupta Efficiency (KGE'). The R score is Pearson's
239 correlation coefficient, ranging between -1 (perfect anti-correlation), and +1 (perfect correlation) highlights the strength of the

https://doi.org/10.5194/egusphere-2025-6351
Preprint. Discussion started: 19 March 2026

linear relationship between two datasets. The proportional bias corresponds to the sum of the differences between the predicted and observed values, normalized by the average of observed values. It ranges between -∞ and +∞, 0 corresponding to no bias. It is computed as follows:

$$PBias = \frac{\sum_{i=1}^{N} (P_i - O_i)}{\sum_{i=1}^{N} O_i} \quad (2)$$

Where P_i refers to a predicted value at time i, and O_i to the reference value at the same timestep. The variability ratio is computed as follows: $\gamma = \frac{\sigma_s/\mu_s}{\sigma_o/\mu_o}$ with $\sigma_s$the standard deviation of the predicted values and σ_o the standard deviation of the reference data. The modified Kling-Gupta Efficiency index (KGE') balances correlation, bias, and variability and is widely used in hydrological studies as a goodness-of-fit criterion. It was proposed by (Kling et al., 2012) as an updated version of the original KGE metric (Gupta et al., 2009) ranging between -∞ and 1, where 1 indicates the perfect fit.

$$KGE' = 1 - \sqrt{(R-1)^2 + (PBias - 1)^2 + (\gamma - 1)^2} \quad (3)$$

Overall, the WMB approach using ERA5 data (WMB1) shows excellent agreement with in situ measurements, yielding a KGE' score of 0.84. In contrast, using GPCC precipitation and ISBA-CTRIP evapotranspiration (WMB2) results in more pronounced discrepancies—both in the annual cycle and higher-frequency variations—leading to a lower KGE' score of 0.53. These results confirm the reliability of the WMB approach for estimating Amazon River discharge and highlight the sensitivity of the method to the choice of datasets used to estimate vertical atmospheric fluxes as shown previously by (Chen et al., 2020)). Biases in net precipitation (P-E), in particular, directly affect the accuracy of discharge estimates.

3.2. Sensitivity of the river discharge to the distance of the gauging station to the outlet

River discharge estimates based on in situ measurements can underestimate the total freshwater flux entering the ocean when gauging stations are located far upstream from the river mouth, as they capture only a portion of the full basin's drainage area. This is the case for the Óbidos station, located approximately 500 km upstream of the Amazon Delta (Fig. 4a). The Water Mass Balance (WMB) approach enables discharge estimation over any drainage area large enough to be resolved by GRACE and GRACE-FO satellite observations. In this study, we compare discharge estimates for the entire Amazon Basin and the Óbidos drainage area using the WMB method, driven by ERA5 atmospheric fluxes—a configuration shown to provide accurate results at Óbidos.

The Óbidos drainage area is approximately 22% smaller than the entire Amazon River Basin, excluding several major tributaries such as the Tapajos, Xingu, and Jari (Fig. 4a). As a result, the mean river discharge at Óbidos is 15% lower than at the river mouth. Similarly, the amplitude of the annual discharge cycle is underestimated by 20% when using data from Óbidos instead of the full basin. Peak flow—defined as the maximum discharge—also shows an underestimation of 15% at Óbidos compared to the river outlet. These discrepancies are substantial and must be considered when assessing the influence of Amazonian freshwater fluxes on the Atlantic Ocean. For context, a 10% underestimation in the Amazon's mean discharge is equivalent to omitting the entire flow of the Mississippi River (Table 1).

https://doi.org/10.5194/egusphere-2025-6351
Preprint. Discussion started: 19 March 2026

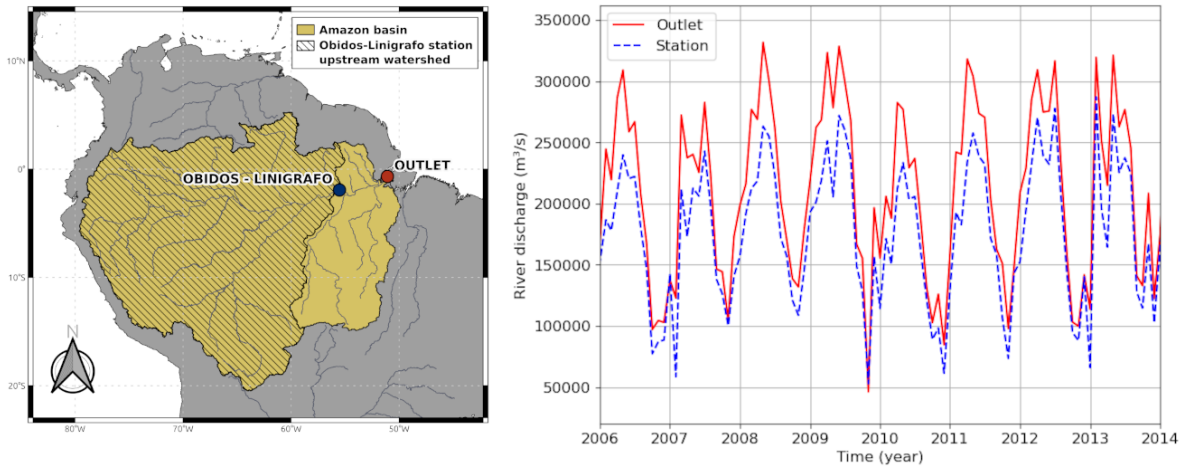

Figure 4: Comparison between discharge values at the Obidos-Linigrafo station located furthest downstream of the Amazon and at the river outlet. Figure (a) shows the location of the Obidos-Linigrafo station as a blue dot and the river outlet as a red dot. The complete river basin is represented in yellow, and the hatched area corresponds to the Obidos-Linigrafo station upstream watershed. Figure (b) displays estimated discharge values using the WMB approach with ERA5 precipitation and evapotranspiration data. The red curve represents the estimation at the outlet location (using the whole river basin), and the blue curve represents the estimation at the Obidos-Linigrafo station (using the station's upstream watershed).

3.3. WMB discharge estimated for 18 major rivers flowing into the Atlantic

River discharge was estimated at the outlet of each of the 18 selected rivers (Fig. 1) using the Water Mass Balance (WMB) approach, driven by two combinations of vertical atmospheric fluxes: ERA5 reanalysis (WMB1), and GPCC precipitation with ISBA evapotranspiration (WMB2) (Table 2). The results show significant discrepancies in both mean discharge and seasonal variability depending on the dataset used to represent atmospheric fluxes.

The largest difference in mean discharge was observed for the Congo River, where WMB2 yielded a discharge of 58,537 m³/s, compared to 27,801 m³/s with WMB1—representing a 53% difference. For smaller rivers, relative differences are even more pronounced. In the Niger River, the choice of dataset results in a 74% difference, while the Magdalena River shows an 87% difference. In extreme cases, such as the São Francisco River, the WMB method produced a negative mean discharge when forced with GPCC and ISBA, clearly highlighting the method's failure to capture river discharge. These discrepancies stem from excessive noise or biases in one or more components of the WMB equation and emphasize the method's sensitivity to the quality of regional atmospheric data.

The largest difference in seasonal discharge amplitude was found in the Amazon River, where the seasonal variation amplitude is overestimated by 56,844 m³/s, or 31% in WMB2 compared to WMB1. Significant differences in seasonal variability were also found between WMB2 and WMB1 for other rivers, such as the Orinoco: 19,506 m³/s (55% of WMB1 amplitude), Mississippi: 13,982 m³/s (48%), and Nelson: 10,909 m³/s (134%) Rivers. Such discrepancies underscore the limitations of the WMB method, which is highly sensitive to uncertainties in atmospheric forcing. Improving the accuracy of net precipitation estimates (P − E) at regional scales would directly enhance the reliability of WMB-based discharge estimates.

https://doi.org/10.5194/egusphere-2025-6351
Preprint. Discussion started: 19 March 2026

While the WMB method is sensitive to the choice of atmospheric forcing data, it offers the significant advantage of enhanced spatial coverage. Specifically, it enables discharge estimates at the outlets of all 18 rivers—whereas in situ gauging stations exist for only 11, and usually not at the river mouths (e.g., Óbidos). Relying solely on these limited observations would lead to an underestimation of the total mean freshwater flux by 21% with respect to the total flux estimated at the outlets, and an underestimation of the seasonal amplitude by 27% (Fig. 5). This estimate is based on river discharge values resulting from the WMB1 approach, considering (i) the full drainage area of all 18 river basins and (ii) the drainage areas corresponding to the 11 gauging stations located closest to the river mouths (Fig. 1).

River name	WMB1		WMB2	
	Mean discharge ($kg/m^3/s$)	Annual amplitude ($kg/m^3/s$)	Mean discharge ($kg/m^3/s$)	Annual amplitude ($kg/m^3/s$)
Amazon	208968	180925	203757	237769
Congo	27801	36903	58537	32961
Orinoco	35054	35381	34393	54887
Mississippi	16054	29418	11430	43400
Parana	18856	23922	20076	22907
Saint-Lawrence	12533	11206	8674	19803
Tocantins	10114	30338	14569	22634
Magdalena	19068	11642	10179	10973
Niger	3349	29246	13084	31139
Uruguay	4403	5232	4372	4997
Ogooue	4248	6635	5228	9623
Cuyuni and Essequibo	2537	5111	2592	6786
Usumacinta	3078	7952	4418	10809
Nelson	3085	8117	2359	19026
Sao Francisco	-1334	7127	3056	9996
Rhine	2442	1898	1524	2353
Mobile	1540	2631	1276	2599
Orange	16	3935	1103	4479
Total	371811	184358	400627	314353

https://doi.org/10.5194/egusphere-2025-6351
Preprint. Discussion started: 19 March 2026

Table 2: Water Mass Balance discharge estimates at river outlets, using the water mass balance approach forced with ERA5 (WMB1) or GPCC and ISBA (WMB2) atmospheric fluxes. Mean seasonal amplitude refers to the difference in discharge between the maximum and minimum value in the mean seasonal cycle. Both the seasonal amplitude and the mean discharge are computed over the 2002—2019 period. The "Total" row refers to the sum of each river time series.

River discharge estimates derived from the WMB approach are subject to significant uncertainties, as evidenced by the large variability associated with the choice of atmospheric forcing data. To further evaluate the method's performance, the river discharge was estimated using the WMB approach over the drainage areas of the 11 selected gauging stations and compared with in situ measurements. The resulting mean and annual discharge amplitudes are listed in Table 3. The amplitude and mean discharge are computed over the longest uninterrupted common interval between the in situ, WMB1 and WMB2 time series. These statistics can therefore not be directly compared between rivers. The "Total" row refers to the sum WMB1 and WMB2 time series over the 11 stations during the 2002—2019 period. As the in situ measurements' time coverage is not consistent between rivers, no total value is provided.

River name	Mean discharge (kg/m^3/s)			Annual amplitude (kg/m^3/s)		
	In situ	WMB1	WMB2	In situ	WMB1	WMB2
Amazon	173434	177495	167785	137590	144549	200581
Congo	39665	27509	57450	25295	35430	30675
Orinoco	33520	30677	30410	65020	31631	49123
Mississippi	21618	16164	9601	21229	25800	38895
Parana	17178	17939	19668	3202	36766	42817
Saint-Lawrence	7345	7409	5005	1501	4643	19098
Tocantins	10068	9616	13996	18965	32664	32820
Niger	5630	1564	10995	12360	31940	30045
Nelson	3891	3105	2326	1120	7716	18433
Rhine	2080	2442	1524	1456	1898	2353
Orange	124	-32	845	213	5587	5519
Total	-	293559	320295	-	133767	266507

Table 3: Intercomparison of the mean and annual discharge values estimated with in situ measurements and with the water mass balance approached forced with ERA5 (WMB1) or GPCC and ISBA (WMB2) atmospheric fluxes. The "Total" row refers to the sum of each river time series.

The largest errors in the mean discharge are obtained for the Congo river which is overestimated by 17 784 m³/s (+ 45%) in WMB2 and underestimated by 12 156 m3/s (-31%) in WMB1. The errors in the mean discharge are generally higher with WMB2, though there are no systematic biases: for some rivers the mean discharge is overestimated (e.g. Congo, Parana, Tocantins, Niger and Orange) and for some others it is underestimated (e.g. Amazon, Orinoco, Mississippi, Saint Lawrence, Nelson, Rhine). The

https://doi.org/10.5194/egusphere-2025-6351
Preprint. Discussion started: 19 March 2026

absolute and relative amplitude of the errors is also variable depending on the river selected. In WMB1, the relative error on the mean river discharge is under 15% for 5 out of 11 rivers, namely the Amazon, Orinoco, Parana, Tocantins and Saint-Lawrence.

Similarly, for the annual cycle, WMB2 generally results in larger deviations from in situ measurements compared to WMB1. The most pronounced errors in the mean annual amplitude occur for the Amazon (+62,991 m³/s, or +46% relative to in situ) and the Parana (+39,615 m³/s, or +1237%) in WMB2. Notable errors are also observed in WMB1, particularly for the Congo (-33,308 m³/s, or -51%), Paraná (+33,564 m³/s, or +1048%) and Niger (+19,580 m³/s, or 158%) Rivers. The error in the annual amplitude of river discharge remains below 15% for only the Amazon, and only when using ERA5 forcing. Once again, no systematic bias is apparent, as both the magnitude and direction of the errors vary depending on the river and the atmospheric dataset used.

The WMB approach is further evaluated using the PBias for the temporal mean, the correlation coefficient (R), the variability ratio (γ), and the modified Kling-Gupta Efficiency (KGE'). All metric values are provided in Table A1 of the Appendix, while PBias and R are illustrated in Fig. 6.

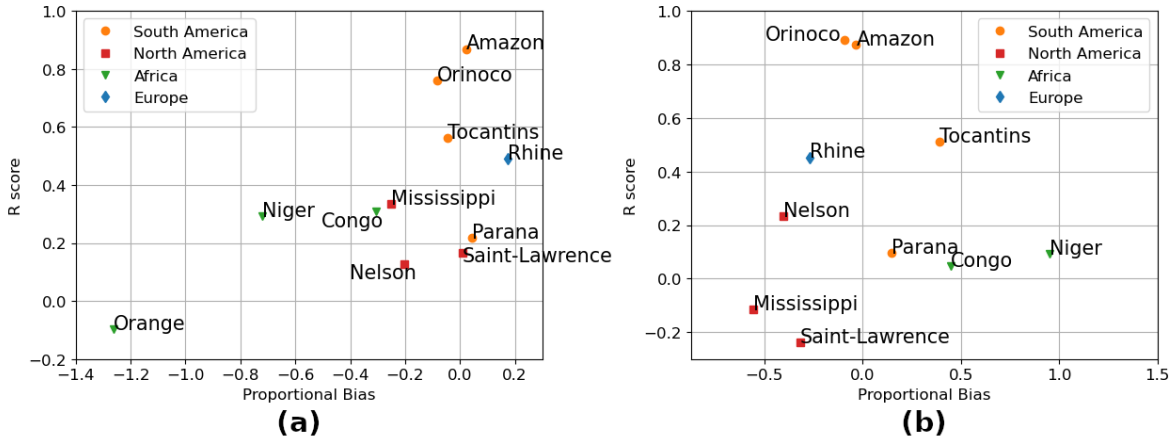

Figure 5: Quality metrics computed at the selected in situ stations by comparing WMB estimates to in situ measurements taken as reference. Figure (a) shows scores for WMB estimates with ERA5 precipitation and ERA5 evapotranspiration. Figure (b) shows scores for WMB estimates with GPCC precipitation and ISBA evapotranspiration. Results for the Orange River are outside of the figure's range with a proportional bias value of 5.80 and an R-score of -0.25.

The WMB approach yields reasonable performance for South American rivers—particularly the Amazon—when forced with ERA5 atmospheric fluxes, as indicated by PBias values close to zero and R scores above 0.5. In contrast, results are more variable and generally less satisfactory for rivers in Africa and North America. Both WMB configurations struggle to capture the mean discharge of African rivers: values are typically underestimated in WMB1 (ranging from -31% to -112%) and overestimated in WMB2 (ranging from +45% to +580%). Overall, the correlation (R score) is higher when using ERA5 than GPCC-ISBA for 8 out of the 11 rivers analyzed.

The variability ratio highlights the substantial high-frequency noise present in the WMB estimates compared to other metrics (PBias, R Score, KGE'). Although the WMB approach generally captures the mean discharge adequately, its high-frequency

https://doi.org/10.5194/egusphere-2025-6351
Preprint. Discussion started: 19 March 2026

variability is considerably greater than that observed in in situ data. Across both atmospheric datasets, the median variability ratio is 2.2 for WMB1 and 1.9 for WMB2.

4 Impact of freshwater fluxes on the Atlantic

In this section, we summarize the results of the impact of the river discharge datasets on the ocean model simulations described in Section 2.4, focusing primarily on salinity fields and then on derived diagnostics.

Figure 7 illustrates the spatial distribution of differences in the mean absolute error (MAE) in sea surface salinity (SSS) across the different model configurations, compared to the EN4 observational dataset (Good et al., 2013). The comparison provides insight into the systematic deviations introduced by each river discharge dataset and highlights the effectiveness of the new WMB-derived river discharge dataset.

The REF experiment, based on the (Dai and Trenberth, 2002) climatology, exhibits significant deviations in regions influenced by major river discharges, particularly in the Amazon plume and along the West African coast. The JRA55-do-driven experiment (J5) displays a somewhat reduced MAE compared to REF, suggesting that its daily varying runoff better captures temporal variability but still lacks improvements in key regions.

The A1 and A2 experiments demonstrate a distinct improvement in MAE, particularly in the western tropical Atlantic and along the equatorial current systems, where freshwater input plays a crucial role in stratification and circulation e.g., (Foltz et al., 2019; Pailler et al., 1999). Both show overall lower MAE values, whose reduction is significant in many regions and equals -0.08 psu and -0.07 psu for A1 and A2, being around -0.04 psu for both S1 and S2, and indicating that using the WMB estimates only for the Amazon, Orinoco, and Tocantis leads to about half of the bias reduction compared to the full WMB dataset.

This implies that the WMB-derived runoff improves the representation of freshwater input into the ocean. The improved consistency with EN4 data suggests that the WMB dataset corrects for biases present in the climatological approach, particularly in regions with high seasonal and interannual variability in discharge. In particular, from the sea surface salinity mean difference of A1 or A2 minus REF (Fig. 6), it appears that both systematically decrease the North Atlantic-wide freshwater input, resulting in an increase in sea surface salinity, whose patterns resemble those of the MAE reduction. There exist only a few areas where the enhanced dataset reduces the surface salinity, confined in the South Atlantic. The differences between the WMB approach using GPCC+ISBA or the ERA5 reanalysis are generally small, and relevant only locally, e.g., in the South-western African coasts (corresponding to the Congo river mouth).

https://doi.org/10.5194/egusphere-2025-6351
Preprint. Discussion started: 19 March 2026

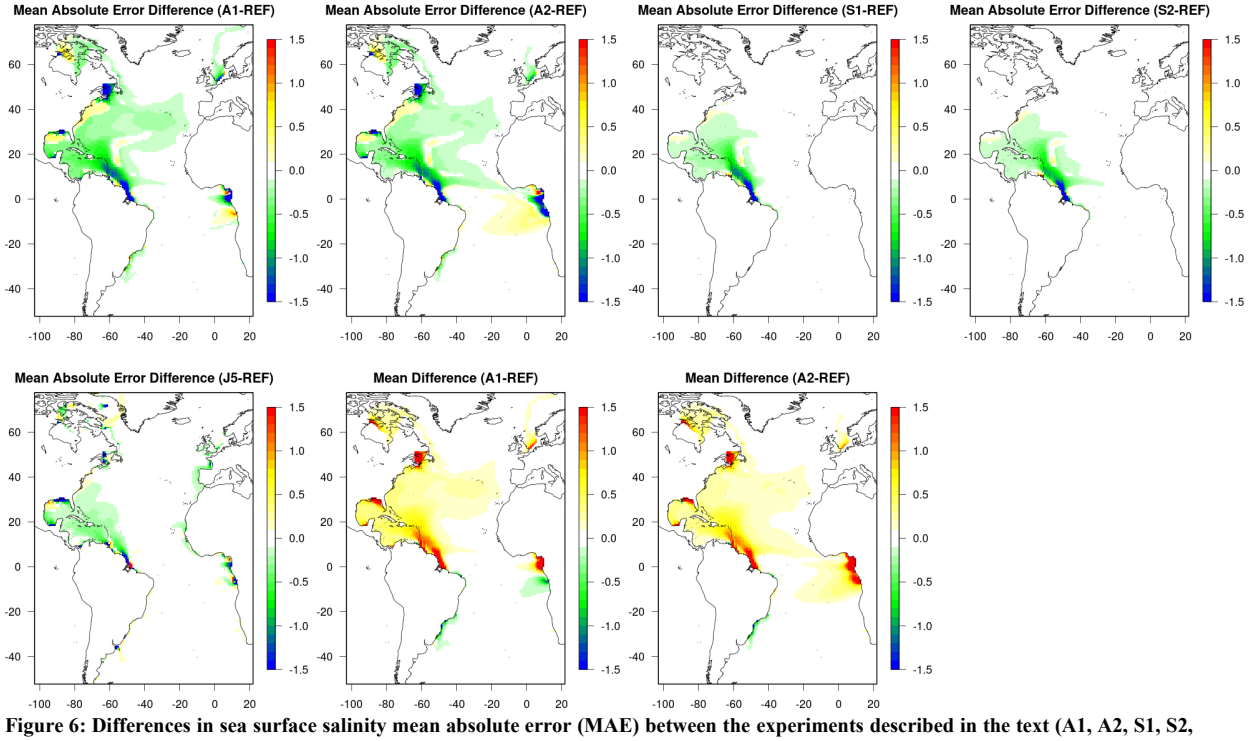

Figure 6: Differences in sea surface salinity mean absolute error (MAE) between the experiments described in the text (A1, A2, S1, S2, J5) and REF. The MAE is computed versus EN4 objective analyses of salinity (Good et al., 2013)**. Negative values indicate a reduction of MAE compared to REF. Panel f, g: time-mean difference of SSS between A1 or A2 and REF. The period is 2003-2020. Units are psu.**

Figure 7 evaluates the root mean square error (RMSE) of salinity as a function of distance from the coast, providing a quantitative assessment of how well the model represents coastal-to-offshore salinity gradients and how far into the open ocean the changes in runoff expand. The REF experiment consistently shows higher RMSE values close to the coast, indicative of the limitations of the monthly climatology in capturing realistic freshwater inputs, combined with its inherent variability therein. On the contrary, the J5 experiment exhibits only moderate improvements near the coastline, likely due to the inclusion of time-varying runoff, although the skill score rapidly worsens towards the open ocean. The A1 and A2 configurations equally demonstrate a notable reduction in RMSE, particularly within the first few hundred kilometers from the coast, indicating a more accurate representation of riverine freshwater distribution. The S1 and S2 experiments confirm localized RMSE reductions, supporting the necessity of accurate basin-scale freshwater modeling around, notably, the Amazon River mouth.

https://doi.org/10.5194/egusphere-2025-6351
Preprint. Discussion started: 19 March 2026

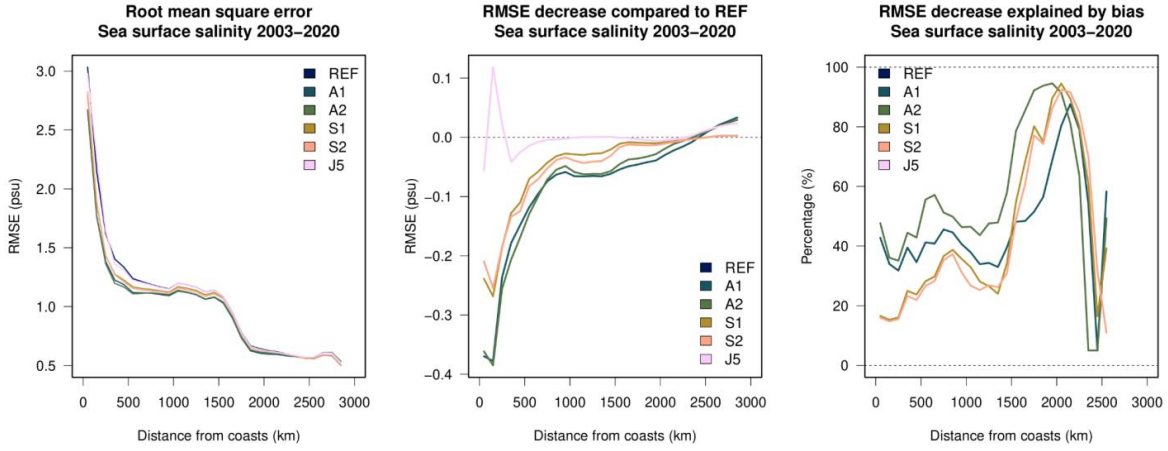

Figure 7: RMSE metrics (2003-2020) as a function of the distance to coast in the North Atlantic Ocean. From left to right: RMSE of the experiments; their RMSE decrease compared to REF; the percentage of RMSE reduction explained by bias reduction.

The RMSE decomposition into systematic (bias-driven) and non-systematic errors (right panel of Fig. 7) highlights that a significant portion of RMSE reduction in the ALL experiment is associated with bias corrections rather than random error reductions. The high percentage of RMSE decrease explained by bias correction suggests that climatological runoff datasets introduced systematic deviations in modeled salinity fields, which the WMB dataset effectively mitigates.

In Fig. 8, we show profiles of Bias and RMSE versus in situ salinity profiles for the gridpoints closer than 500km to the shoreline. This figure provides an assessment of the vertical structure of salinity biases and RMSE compared to EN4 data (Good et al., 2013), offering insights into how different runoff configurations affect subsurface salinity distribution. The REF experiment shows a pronounced fresh bias in the upper layers. The J5 experiment partially reduces surface bias but still exhibits deviations at intermediate depths; while S1, S2 provide an intermediate solution, A1 and A2 significantly reduce the fresh bias in the surface layer, bringing salinity profiles closer to observations, with improvements extending into the subsurface layers, namely extending to ~100m depth. The overall RMSE reduction in the top 100 m of depth is equal to 11%, 10%, 5%, 5%, and 5%, for A1, A2, S1, S2 and J5, respectively, suggesting that the use of GPCC+ISBA slightly outperforms the use of land freshwater fluxes from ERA5.

The largest RMSE values are concentrated in the upper ocean (halocline), where riverine freshwater influences are most pronounced. The A1 and A2 experiments reduce RMSE not only at the surface but also at intermediate depths, suggesting a more realistic penetration of freshwater input into the ocean interior. The systematic error reduction across depths indicates that the positive impact of the WMB dataset penetrates through the upper ocean, potentially leading to a more physically consistent representation of vertical stratification. Slight improvements were also found in sea surface temperature, with a reduction of MAE of the order of 0.1°C or less; however, changes in SST are not statistically significant and are not shown, although recent studies outline possible mechanisms of the changes of coastal stratification on the SST (Aroucha et al., 2025).

https://doi.org/10.5194/egusphere-2025-6351
Preprint. Discussion started: 19 March 2026

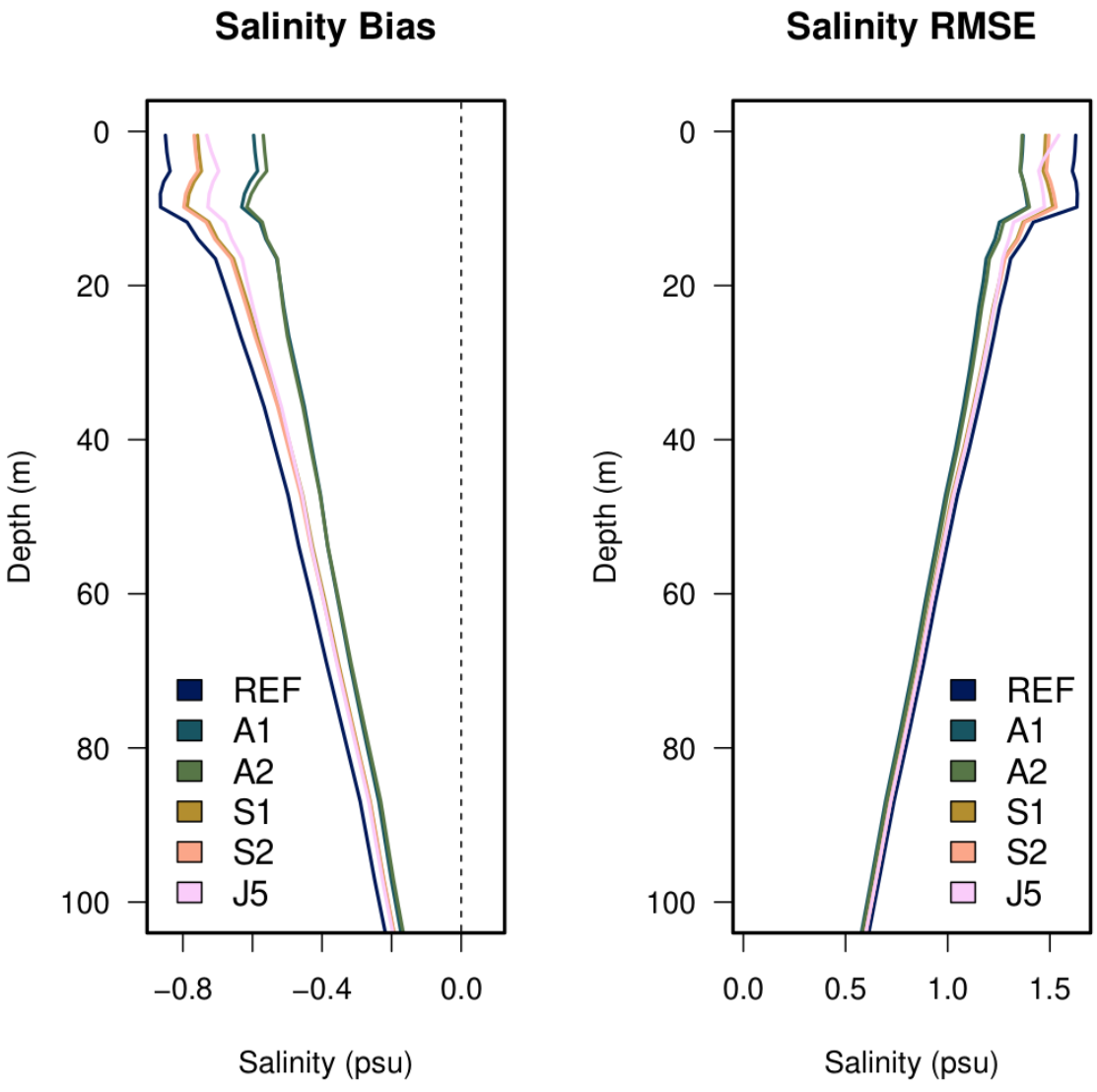

Figure 8: Salinity bias and RMSE profiles for the experiments presented in the text, calculated against EN4 objective analyses of salinity (Good et al., 2013), for the period 2003-2020. Only gridpoints closer than 500km to the shoreline are used.

The introduction of the WMB-derived river discharge dataset leads to an increase in salinity compared to the REF experiment, especially in the Amazon plume and other freshwater-influenced regions. This modification affects ocean stratification and upper-ocean mixing, and subsequently impacts large-scale circulation and meridional transport. In A1, increased sea surface salinity and weaker stratification enhance vertical mixing, which redistributes momentum across a deeper ocean layer. This leads to a reduction in upper-ocean current speeds, downstream of the Amazon River discharge and other river mouths, counteracting enhanced circulation upstream. This is visible in Fig. 9, which shows the mean current speed for ALL (left panel) and the mean difference between ALL and REF (right panel).

https://doi.org/10.5194/egusphere-2025-6351
Preprint. Discussion started: 19 March 2026

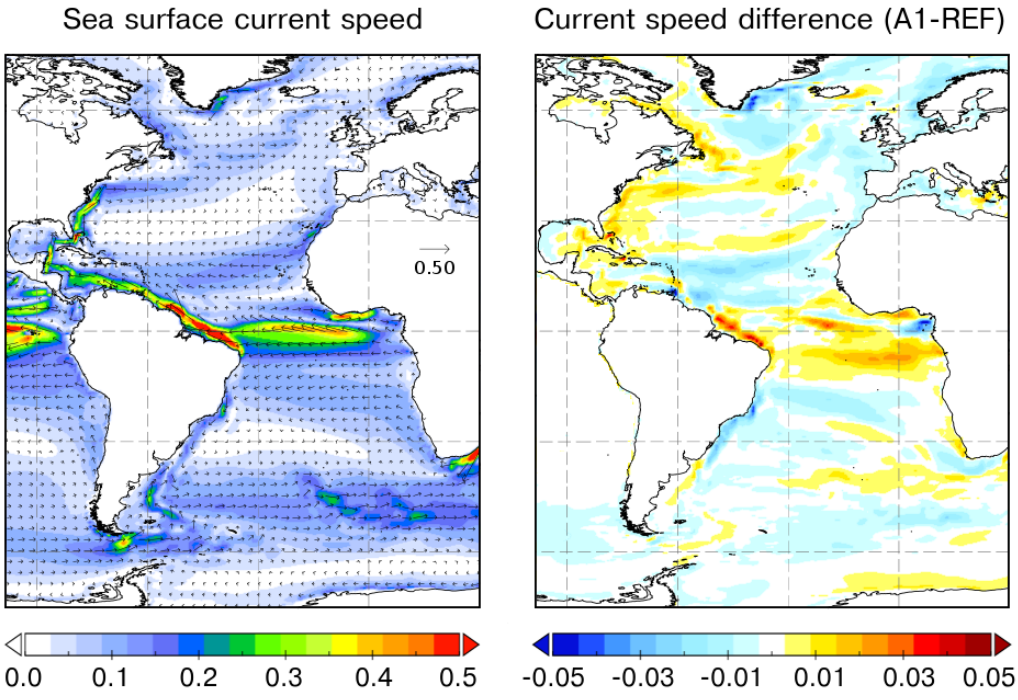

Figure 9: Mean sea surface current in the North Atlantic Ocean for A1 (left panel) and difference between A1 and REF (right panel), over the period 2003-2020. Units are m s^{-1}.

Additionally, the reduced freshwater input in A1 and A2 weakens the horizontal density gradients, possibly causing more direct northward transport along the coast and reducing the strength of the North Brazil Current retroflection, and enhancing the interaction with the North Equatorial Countercurrent (NECC), which transports water eastward towards the Atlantic cold tongue, as in general less freshwater-driven stratification allows for larger net meridional exchanges.

These mechanisms are indeed associated with an increase of meridional transports in the South and Equatorial Atlantic (up to about 15°N) and a slight decrease of transports north of 15°N, visible in Fig. 10. Although relatively small in absolute numbers, modifications to the riverine inputs consistently modify the meridional redistribution of mass, heat, and freshwater across the Atlantic Ocean. No significant impact is found on the thermohaline overturning circulation (not shown), although the relative shortness of the experiments, imposed by gravimeter data availability, may conceal the impact of the freshwater on low-frequency thermohaline circulation.

https://doi.org/10.5194/egusphere-2025-6351
Preprint. Discussion started: 19 March 2026

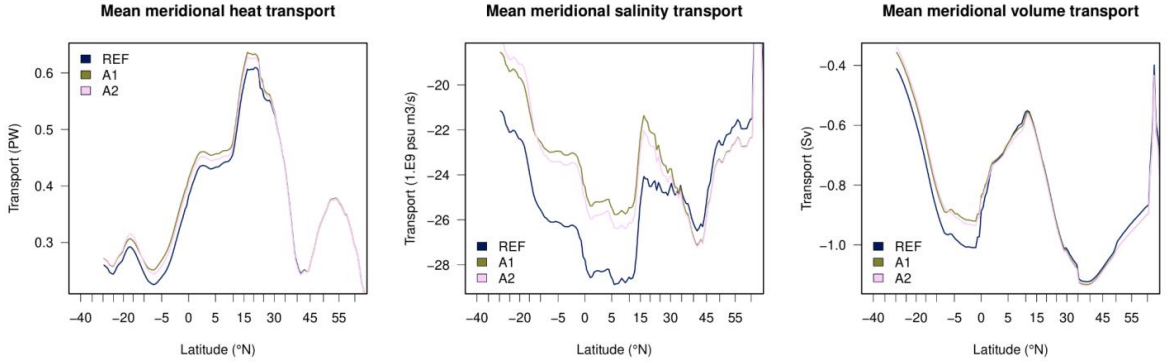

Figure 10: Meridional volume, heat, and salinity transports across the Atlantic Ocean, for the A1, A2, and REF experiments over the 2003-2020 period.

5 Conclusions and Perspectives

Freshwater fluxes play a crucial role in the ocean salinity, circulation, and sea level variability, and yet are often poorly represented in general ocean circulation models. This study uses the Water Mass Balance (WMB) approach, combining satellite gravimetry and atmospheric data, to estimate river discharge. The comparison of the WMB approach to in situ measurements has shown mitigated potential for estimating freshwater discharge into the Atlantic Ocean.

For the Amazon River—the largest contributor of freshwater to the Atlantic—the WMB method closely reproduces in situ measurements at the Óbidos station, capturing both seasonal and long-term trends with a high correlation coefficient ($R \approx 0.88$) and a Kling-Gupta Efficiency (KGE') score of 0.84. Importantly, the WMB approach enables discharge estimation at the river outlet and captures full basin contributions more accurately than upstream gauges like Óbidos, avoiding substantial underestimation of freshwater fluxes.

At a broader scale, the WMB method enabled freshwater flux estimation across 18 major Atlantic-draining river basins, demonstrating good spatial coverage and strong agreement with in situ data for several South American rivers. ERA5 atmospheric forcing consistently outperformed the GPCC–ISBA combination, with lower mean biases and better correlation across most basins.

However, strong regional limitations persist: the WMB method performs less reliably over African and North American rivers, where biases in atmospheric reanalyses can lead to significant errors in both mean discharge and seasonal amplitude. Additionally, WMB river discharge estimates exhibited exaggerated high-frequency variability, especially when using GPCC–ISBA forcing, reflecting noise sensitivity and uncertainty in net precipitation estimates.

Despite these limitations in the WMB approach, the improved salinity representation in the A1 and A2 experiments indicates that freshwater processes are better captured. Using all Atlantic river drainage basin data, RMSE is reduced near the coast, confirming that the WMB dataset improves the representation of riverine freshwater dispersal. Bias correction is the dominant factor in RMSE reduction, reinforcing the systematic improvements provided by the new dataset. Furthermore, the WMB-derived dataset improves salinity biases not only at the surface but also at depth, enhancing the realism of ocean stratification (see also, e.g., (Aroucha et al., 2025)). The use of GPCC+ISBA freshwater fluxes in the WMB formulation slightly outperforms the use of the ERA5 fluxes, with

https://doi.org/10.5194/egusphere-2025-6351
Preprint. Discussion started: 19 March 2026

an RMSE reduction of 11% and 10%, respectively, compared to using the climatological runoff. Furthermore, the adoption of only three high-confidence river discharge estimates (Amazon, Orinoco, and Tocantis) leads to about half of the error reduction compared to the full 18-river dataset.

Given that ocean salinity affects density stratification and mixing, these improvements have downstream impacts on ocean circulation, thermocline structure, and regional climate variability. We have shown in particular the associated changes in reduced vertical stratification, enhanced upper ocean circulation, and meridional transports. These findings highlight the importance of accurate river discharge datasets, aligning with previous studies emphasizing the role of riverine inputs in shaping upper-ocean dynamics ((Chandanpurkar et al., 2022; Feng et al., 2021)). The improved salinity representation has implications for ocean circulation, stratification, climate modeling, and biogeochemical cycles, reinforcing the need for continued refinement of freshwater flux datasets.

In summary, the WMB approach, particularly when constrained with ERA5 atmospheric data, is a promising tool for improving ocean model forcing in regions lacking dense hydrological monitoring. Nevertheless, its accuracy is highly dependent on the quality of atmospheric flux inputs and remains limited by coarse spatial resolution and noise, especially in smaller or poorly monitored basins. Continued improvement in satellite data integration and regional flux estimation is essential to enhance its robustness across diverse hydrological settings. Artificial intelligence techniques could further enhance performance by integrating in situ measurements with the WMB approach to better identify sources of bias and error. Significant improvements are anticipated with future NGGM (Next Generation Gravity Mission) and MAGIC (Mass change And Geosciences International Constellation) satellite gravity missions, aiming at delivering higher spatial and temporal resolution, reduced uncertainties, and lower data latency in gravity field observations.

Appendix A

Metric	R (correlation)		γ (Variability ratio)		PBias		KGE'	
Atmospheric dataset	WMB1	WMB2	WMB1	WMB2	WMB1	WMB2	WMB1	WMB2
Amazon	0.87	0.88	1.08	1.45	0.02	-0.03	0.84	0.53
Congo	0.31	0.05	3.41	1.37	-0.31	0.45	-1.52	-0.12
Orinoco	0.76	0.89	0.66	0.89	-0.08	-0.09	0.57	0.82
Mississippi	0.33	-0.11	2.20	3.92	-0.25	-0.56	-0.40	-2.17
Parana	0.22	0.10	6.80	6.21	0.04	0.14	-4.85	-4.29
Saint-Lawrence	0.17	-0.24	6.30	13.23	0.01	-0.32	-4.37	-11.30
Tocantins	0.56	0.51	2.03	1.17	-0.04	0.39	-0.12	0.35
Niger	0.29	0.09	9.05	1.24	-0.72	0.95	-7.11	-0.34

https://doi.org/10.5194/egusphere-2025-6351
Preprint. Discussion started: 19 March 2026

Nelson	0.13	0.23	7.22	11.68	-0.20	-0.40	-5.28	-9.72
Rhine	0.49	0.45	2.03	3.07	0.17	-0.27	-0.16	-1.16
Orange	-0.10	-0.25	-55.52	1.89	-1.26	5.80	-55.54	-5.00

Table A1: Several dimensionless quality metrics computed at the selected in situ stations by comparing WMB estimates to in situ measurements taken as reference.

Data availability

Discharge time series estimated with the Water Mass Balance approach (WMB1 and WMB2) at the outlet for each river are available online at: https://doi.org/10.5281/zenodo.17589359

Author contribution

LK, TV, JP, CSz, GG and CSi collected and curated the input data to the discharge estimates. LK, TV, JP and CSz produced the discharge timeseries. AS and CY performed the impact analysis on the ocean model. The manuscript was primarily written by LK, TV, JP and AS, with contributions and comments from the other coauthors.

Competing interests

The authors declare that they have no conflict of interest.

Acknowledgements

This work has been carried out as part of the Copernicus Marine Service WAMBOR and F^{3}O projects. Copernicus Marine Service is implemented by Mercator Ocean in the framework of a delegation agreement with the European Union.

References

Catalogue – Hybam: https://hybam.obs-mip.fr/catalogue/?currentSelection=a6e2e07a-de59-30f5-9a97-e6e7ef0cdc98, last access: 29 August 2025.

Aroucha, L. C., Lübbecke, J. F., Brandt, P., Schwarzkopf, F. U., and Biastoch, A.: River discharge impacts coastal southeastern tropical Atlantic sea surface temperature and circulation: a model-based analysis, Ocean Sci., 21, 661–678, https://doi.org/10.5194/os-21-661-2025, 2025.

Bernard, B., Madec, G., Penduff, T., Molines, J.-M., Treguier, A.-M., Le Sommer, J., Beckmann, A., Biastoch, A., Böning, C., Dengg, J., Derval, C., Durand, E., Gulev, S., Remy, E., Talandier, C., Theetten, S., Maltrud, M., McClean, J., and De Cuevas, B.: Impact of partial steps and momentum advection schemes in a global ocean circulation model at eddy-permitting resolution, Ocean Dyn., 56, 543–567, https://doi.org/10.1007/s10236-006-0082-1, 2006.

Blazquez, A., Meyssignac, B., Lemoine, J., Berthier, E., Ribes, A., and Cazenave, A.: Exploring the uncertainty in GRACE estimates of the mass redistributions at the Earth surface: implications for the global water and sea level budgets, Geophys. J.

Int., 215, 415–430, https://doi.org/10.1093/gji/ggy293, 2018.

Bourdalle-Badie and Treguier: Mercator-Ocean Report. A Climatology of Runoff for the Global Ocean-Ice Model ORCA025; Technical Report MOO-RP-425-365-MER; Mercator Ocean, 2006.

Brodeau, L., Barnier, B., Gulev, S. K., and Woods, C.: Climatologically Significant Effects of Some Approximations in the Bulk Parameterizations of Turbulent Air–Sea Fluxes, J. Phys. Oceanogr., 47, 5–28, https://doi.org/10.1175/JPO-D-16-0169.1, 2017.

Cáceres, D., Marzeion, B., Malles, J. H., Gutknecht, B. D., Müller Schmied, H., and Döll, P.: Assessing global water mass transfers from continents to oceans over the period 1948–2016, Hydrol. Earth Syst. Sci., 24, 4831–4851, https://doi.org/10.5194/hess-24-4831-2020, 2020.

Caron, L., Ivins, E. R., Larour, E., Adhikari, S., Nilsson, J., and Blewitt, G.: GIA Model Statistics for GRACE Hydrology, Cryosphere, and Ocean Science, Geophys. Res. Lett., 45, 2203–2212, https://doi.org/10.1002/2017GL076644, 2018.

Chandanpurkar, H. A., Lee, T., Wang, X., Zhang, H., Fournier, S., Fenty, I., Fukumori, I., Menemenlis, D., Piecuch, C. G., Reager, J. T., Wang, O., and Worden, J.: Influence of Nonseasonal River Discharge on Sea Surface Salinity and Height, J. Adv. Model. Earth Syst., 14, e2021MS002715, https://doi.org/10.1029/2021MS002715, 2022.

Chen, J., Tapley, B., Wilson, C., Cazenave, A., Seo, K.-W., and Kim, J.-S.: Global Ocean Mass Change From GRACE and GRACE Follow-On and Altimeter and Argo Measurements, Geophys. Res. Lett., 47, e2020GL090656, https://doi.org/10.1029/2020GL090656, 2020.

Cheng, M., Tapley, B. D., and Ries, J. C.: Deceleration in the Earth's oblateness, J. Geophys. Res. Solid Earth, 118, 740–747, https://doi.org/10.1002/jgrb.50058, 2013.

Crétaux, J.-F., Abarca-del-Río, R., Bergé-Nguyen, M., Arsen, A., Drolon, V., Clos, G., and Maisongrande, P.: Lake Volume Monitoring from Space, Surv. Geophys., 37, 269–305, https://doi.org/10.1007/s10712-016-9362-6, 2016.

Dai, A.: Dai and Trenberth Global River Flow and Continental Discharge Dataset, 2017.

Dai, A. and Trenberth, K. E.: Estimates of Freshwater Discharge from Continents: Latitudinal and Seasonal Variations, J. Hydrometeorol., 3, 660–687, https://doi.org/10.1175/1525-7541(2002)003%253C0660:EOFDFC%253E2.0.CO;2, 2002.

Dai, A., Qian, T., Trenberth, K. E., and Milliman, J. D.: Changes in Continental Freshwater Discharge from 1948 to 2004, J. Clim., 22, 2773–2792, https://doi.org/10.1175/2008JCLI2592.1, 2009.

Decharme, B., Delire, C., Minvielle, M., Colin, J., Vergnes, J.-P., Alias, A., Saint-Martin, D., Séférian, R., Sénési, S., and Voldoire, A.: Recent Changes in the ISBA-CTRIP Land Surface System for Use in the CNRM-CM6 Climate Model and in Global Off-Line Hydrological Applications, J. Adv. Model. Earth Syst., 11, 1207–1252, https://doi.org/10.1029/2018ms001545, 2019.

Dobriyal, P., Badola, R., Tuboi, C., and Hussain, S. A.: A review of methods for monitoring streamflow for sustainable water resource management, Appl. Water Sci., 7, 2617–2628, https://doi.org/10.1007/s13201-016-0488-y, 2017.

Dobslaw, H. and Thomas, M.: Simulation and observation of global ocean mass anomalies, J. Geophys. Res. Oceans, 112, https://doi.org/10.1029/2006JC004035, 2007.

Elmi, O., Tourian, M. J., Saemian, P., and Sneeuw, N.: Remote Sensing-Based Extension of GRDC Discharge Time Series - A Monthly Product with Uncertainty Estimates, Sci. Data, 11, 240, https://doi.org/10.1038/s41597-024-03078-6, 2024.

Feng, Y., Menemenlis, D., Xue, H., Zhang, H., Carroll, D., Du, Y., and Wu, H.: Improved representation of river runoff in Estimating the Circulation and Climate of the Ocean Version 4 (ECCOv4) simulations: implementation, evaluation, and impacts to coastal plume regions, Geosci. Model Dev., 14, 1801–1819, https://doi.org/10.5194/gmd-14-1801-2021, 2021.

Foltz, G. R., Brandt, P., Richter, I., Rodríguez-Fonseca, B., Hernandez, F., Dengler, M., Rodrigues, R. R., Schmidt, J. O., Yu, L., Lefevre, N., Da Cunha, L. C., McPhaden, M. J., Araujo, M., Karstensen, J., Hahn, J., Martín-Rey, M., Patricola, C. M., Poli, P., Zuidema, P., Hummels, R., Perez, R. C., Hatje, V., Lübbecke, J. F., Polo, I., Lumpkin, R., Bourlès, B., Asuquo, F. E., Lehodey, P., Conchon, A., Chang, P., Dandin, P., Schmid, C., Sutton, A., Giordani, H., Xue, Y., Illig, S., Losada, T., Grodsky, S. A.,

https://doi.org/10.5194/egusphere-2025-6351
Preprint. Discussion started: 19 March 2026

Gasparin, F., Lee, T., Mohino, E., Nobre, P., Wanninkhof, R., Keenlyside, N., Garcon, V., Sánchez-Gómez, E., Nnamchi, H. C., Drévillon, M., Storto, A., Remy, E., Lazar, A., Speich, S., Goes, M., Dorrington, T., Johns, W. E., Moum, J. N., Robinson, C., Perruche, C., de Souza, R. B., Gaye, A. T., López-Parages, J., Monerie, P.-A., Castellanos, P., Benson, N. U., Hounkonnou, M. N., Duhá, J. T., Laxenaire, R., and Reul, N.: The Tropical Atlantic Observing System, Front. Mar. Sci., 6, https://doi.org/10.3389/fmars.2019.00206, 2019.

Fournier, S., Reager, J. T., Chandanpurkar, H. A., Pascolini-Campbell, M., and Jarugula, S.: The Salinity of Coastal Waters as a Bellwether for Global Water Cycle Changes, Geophys. Res. Lett., 50, e2023GL106684, https://doi.org/10.1029/2023GL106684, 2023.

Gaspar, P., Grégoris, Y., and Lefevre, J.-M.: A simple eddy kinetic energy model for simulations of the oceanic vertical mixing: Tests at station Papa and long-term upper ocean study site, J. Geophys. Res. Oceans, 95, 16179–16193, https://doi.org/10.1029/JC095iC09p16179, 1990.

Good, S. A., Martin, M. J., and Rayner, N. A.: EN4: Quality controlled ocean temperature and salinity profiles and monthly objective analyses with uncertainty estimates, J. Geophys. Res. Oceans, 118, 6704–6716, https://doi.org/10.1002/2013JC009067, 2013.

GRDC: GRDC Major River Basins. Global Runoff Data Centre. 2nd, rev. ed. Koblenz: Federal Institute of Hydrology (BfG), 2020.

Gupta, H. V., Kling, H., Yilmaz, K. K., and Martinez, G. F.: Decomposition of the mean squared error and NSE performance criteria: Implications for improving hydrological modelling, J. Hydrol., 377, 80–91, https://doi.org/10.1016/j.jhydrol.2009.08.003, 2009.

Hamlington, B. D., Gardner, A. S., Ivins, E., Lenaerts, J. T. M., Reager, J. T., Trossman, D. S., Zaron, E. D., Adhikari, S., Arendt, A., Aschwanden, A., Beckley, B. D., Bekaert, D. P. S., Blewitt, G., Caron, L., Chambers, D. P., Chandanpurkar, H. A., Christianson, K., Csatho, B., Cullather, R. I., DeConto, R. M., Fasullo, J. T., Frederikse, T., Freymueller, J. T., Gilford, D. M., Girotto, M., Hammond, W. C., Hock, R., Holschuh, N., Kopp, R. E., Landerer, F., Larour, E., Menemenlis, D., Merrifield, M., Mitrovica, J. X., Nerem, R. S., Nias, I. J., Nieves, V., Nowicki, S., Pangaluru, K., Piecuch, C. G., Ray, R. D., Rounce, D. R., Schlegel, N., Seroussi, H., Shirzaei, M., Sweet, W. V., Velicogna, I., Vinogradova, N., Wahl, T., Wiese, D. N., and Willis, M. J.: Understanding of Contemporary Regional Sea-Level Change and the Implications for the Future, Rev. Geophys., 58, https://doi.org/10.1029/2019RG000672, 2020.

Hersbach, H., Bell, B., Berrisford, P., Hirahara, S., Horányi, A., Muñoz-Sabater, J., Nicolas, J., Peubey, C., Radu, R., Schepers, D., Simmons, A., Soci, C., Abdalla, S., Abellan, X., Balsamo, G., Bechtold, P., Biavati, G., Bidlot, J., Bonavita, M., De Chiara, G., Dahlgren, P., Dee, D., Diamantakis, M., Dragani, R., Flemming, J., Forbes, R., Fuentes, M., Geer, A., Haimberger, L., Healy, S., Hogan, R. J., Hólm, E., Janisková, M., Keeley, S., Laloyaux, P., Lopez, P., Lupu, C., Radnoti, G., de Rosnay, P., Rozum, I., Vamborg, F., Villaume, S., and Thépaut, J.-N.: The ERA5 global reanalysis, Q. J. R. Meteorol. Soc., 146, 1999–2049, https://doi.org/10.1002/qj.3803, 2020.

Huang, B. and Mehta, V. M.: Influences of freshwater from major rivers on global ocean circulation and temperatures in the MIT ocean general circulation model, Adv. Atmospheric Sci., 27, 455–468, https://doi.org/10.1007/s00376-009-9022-6, 2010.

Jahfer, S., Vinayachandran, P. N., and Nanjundiah, R. S.: Long-term impact of Amazon river runoff on northern hemispheric climate, Sci. Rep., 7, 10989, https://doi.org/10.1038/s41598-017-10750-y, 2017.

Kling, H., Fuchs, M., and Paulin, M.: Runoff conditions in the upper Danube basin under an ensemble of climate change scenarios, J. Hydrol., 424–425, 264–277, https://doi.org/10.1016/j.jhydrol.2012.01.011, 2012.

Kusche, J., Schmidt, R., Petrovic, S., and Rietbroek, R.: Decorrelated GRACE time-variable gravity solutions by GFZ, and their validation using a hydrological model, J. Geod., 83, 903–913, https://doi.org/10.1007/s00190-009-0308-3, 2009.

Landerer, F. W., Flechtner, F. M., Save, H., Webb, F. H., Bandikova, T., Bertiger, W. I., Bettadpur, S. V., Byun, S. H., Dahle, C., Dobslaw, H., Fahnestock, E., Harvey, N., Kang, Z., Kruizinga, G. L. H., Loomis, B. D., McCullough, C., Murböck, M., Nagel, P., Paik, M., Pie, N., Poole, S., Strekalov, D., Tamisiea, M. E., Wang, F., Watkins, M. M., Wen, H.-Y., Wiese, D. N., and Yuan, D.-N.: Extending the Global Mass Change Data Record: GRACE Follow-On Instrument and Science Data Performance, Geophys. Res. Lett., 47, e2020GL088306, https://doi.org/10.1029/2020GL088306, 2020.

Large, W. G. and Yeager, S. G.: The global climatology of an interannually varying air–sea flux data set, Clim. Dyn., 33, 341–

364, https://doi.org/10.1007/s00382-008-0441-3, 2009.

Lehner, B. and Grill, G.: Global river hydrography and network routing: baseline data and new approaches to study the world's large river systems, Hydrol. Process., 27, 2171–2186, https://doi.org/10.1002/hyp.9740, 2013.

Lemoine, J. and Reinquin, F.: Processing of SLR observations at CNES, Newsl. EGSIEM, 3, 2017.

Loomis, B. D., Rachlin, K. E., and Luthcke, S. B.: Improved Earth Oblateness Rate Reveals Increased Ice Sheet Losses and Mass-Driven Sea Level Rise, Geophys. Res. Lett., 46, 6910–6917, https://doi.org/10.1029/2019GL082929, 2019.

Madec, G., Bourdallé-Badie, R., Pierre-Antoine Bouttier, Bricaud, C., Bruciaferri, D., Calvert, D., Chanut, J., Clementi, E., Coward, A., Delrosso, D., Ethé, C., Flavoni, S., Graham, T., Harle, J., Iovino, D., Lea, D., Lévy, C., Lovato, T., Martin, N., Masson, S., Mocavero, S., Paul, J., Rousset, C., Storkey, D., Storto, A., and Vancoppenolle, M.: NEMO ocean engine, https://doi.org/10.5281/ZENODO.1472492, 2017.

Pailler, K., Bourlès, B., and Gouriou, Y.: The barrier layer in the western tropical Atlantic Ocean, Geophys. Res. Lett., 26, 2069–2072, https://doi.org/10.1029/1999GL900492, 1999.

Peltier, W. R., Argus, D. F., and Drummond, R.: Comment on "An Assessment of the ICE-6G_C (VM5a) Glacial Isostatic Adjustment Model" by Purcell et al., J. Geophys. Res. Solid Earth, 123, 2019–2028, https://doi.org/10.1002/2016JB013844, 2018.

Pfeffer, J., Cazenave, A., and Barnoud, A.: Analysis of the interannual variability in satellite gravity solutions: detection of climate modes fingerprints in water mass displacements across continents and oceans, Clim. Dyn., 58, 1065–1084, https://doi.org/10.1007/s00382-021-05953-z, 2022.

Sausen, R., Schubert, S., and Dümenil, L.: A model of river runoff for use in coupled atmosphere-ocean models, J. Hydrol., 155, 337–352, https://doi.org/10.1016/0022-1694(94)90177-5, 1994.

Schneider, U., Becker, A., Finger, P., Meyer-Christoffer, A., Rudolf, B., and Ziese, M.: GPCC Full Data Reanalysis Version 7.0 at 0.5°: Monthly Land-Surface Precipitation from Rain-Gauges built on GTS-based and Historic Data: Gridded Monthly Totals (7.0), https://doi.org/10.5676/DWD_GPCC/FD_M_V7_050, 2015.

Storto, A. and Yang, C.: Acceleration of the ocean warming from 1961 to 2022 unveiled by large-ensemble reanalyses, Nat. Commun., 15, 545, https://doi.org/10.1038/s41467-024-44749-7, 2024.

Storto, A., Bonaduce, A., Feng, X., and Yang, C.: Steric Sea Level Changes from Ocean Reanalyses at Global and Regional Scales, Water, 11, 1987, https://doi.org/10.3390/w11101987, 2019.

Sun, Y., Riva, R., and Ditmar, P.: Optimizing estimates of annual variations and trends in geocenter motion and J2 from a combination of GRACE data and geophysical models, J. Geophys. Res. Solid Earth, 121, 8352–8370, https://doi.org/10.1002/2016JB013073, 2016.

Syed, T. H., Famiglietti, J. S., Chen, J., Rodell, M., Seneviratne, S. I., Viterbo, P., and Wilson, C. R.: Total basin discharge for the Amazon and Mississippi River basins from GRACE and a land-atmosphere water balance, Geophys. Res. Lett., 32, https://doi.org/10.1029/2005GL024851, 2005.

Syed, T. H., Famiglietti, J. S., and Chambers, D. P.: GRACE-Based Estimates of Terrestrial Freshwater Discharge from Basin to Continental Scales, J. Hydrometeorol., 10, 22–40, https://doi.org/10.1175/2008JHM993.1, 2009.

Tajouri, S., Llovel, W., Sévellec, F., Molines, J.-M., Mathiot, P., Penduff, T., and Leroux, S.: Simulated Impact of Time-Varying River Runoff and Greenland Freshwater Discharge on Sea Level Variability in the Beaufort Gyre Over 2005–2018, J. Geophys. Res. Oceans, 129, e2024JC021237, https://doi.org/10.1029/2024JC021237, 2024.

Tapley, B. D., Bettadpur, S., Watkins, M., and Reigber, C.: The gravity recovery and climate experiment: Mission overview and early results, Geophys. Res. Lett., 31, n/a-n/a, https://doi.org/10.1029/2004gl019920, 2004.

Thouvenin-Masson, C., Boutin, J., Échevin, V., Lazar, A., and Vergely, J.-L.: Influence of river runoff and precipitation on the seasonal and interannual variability of sea surface salinity in the eastern North Tropical Atlantic, Ocean Sci., 20, 1547–1566,

https://doi.org/10.5194/egusphere-2025-6351
Preprint. Discussion started: 19 March 2026

673 https://doi.org/10.5194/os-20-1547-2024, 2024.

674 Tsujino, H., Urakawa, S., Nakano, H., Small, R. J., Kim, W. M., Yeager, S. G., Danabasoglu, G., Suzuki, T., Bamber, J. L.,
675 Bentsen, M., Böning, C. W., Bozec, A., Chassignet, E. P., Curchitser, E., Boeira Dias, F., Durack, P. J., Griffies, S. M., Harada,
676 Y., Ilicak, M., Josey, S. A., Kobayashi, C., Kobayashi, S., Komuro, Y., Large, W. G., Le Sommer, J., Marsland, S. J., Masina, S.,
677 Scheinert, M., Tomita, H., Valdivieso, M., and Yamazaki, D.: JRA-55 based surface dataset for driving ocean–sea-ice models
678 (JRA55-do), Ocean Model., 130, 79–139, https://doi.org/10.1016/j.ocemod.2018.07.002, 2018.

679 Vaujour, T., Kern, L., Pfeffer, J., Storto, A., Szczypta, C., Garric, G., Sirere, C., Larnicol, G., YANG, C., Bourdallé-Badie, R.,
680 and Guinehut, S.: River discharge estimates for 18 major Atlantic rivers using the Water Mass Balance approach,
681 https://doi.org/10.5281/zenodo.17589359, 2025.